

Assimilation of microwave imagers (GCOM-W1/AMSR2, GPM/GMI)

Masahiro Kazumori

*Japan Meteorological Agency
kazumori@met.kishou.go.jp*

ABSTRACT

This paper describes assimilation of microwave imagers in NWP systems. Progress in ocean emissivity modelling for the microwave imager radiance assimilation is shown. Recent progress for utilization of new microwave imagers (the Global Change Observation Mission (GCOM)-Water 1/ Advanced Microwave Scanning Radiometer 2 (AMSR2) and Global Precipitation Measurement (GPM)/GPM Microwave Imager (GMI)) is shown with results from data assimilation experiments in European Centre for Medium-Range Weather Forecasts (ECMWF) and Japan Meteorological Agency (JMA).

1 Introduction

Space-based microwave imager observations have become an indispensable part of global Earth Observing System (EOS). In data assimilations for numerical weather predictions (NWP), the information obtained from the microwave imagers helps improve atmospheric humidity, cloud and precipitation analyses and forecasts. Operational NWP centres have been utilizing these information from radiance data of Defense Meteorological Satellite Program (DMSP) satellite Special Sensor Microwave Imager Sounder (SSMIS), The Tropical Rainfall Measuring Mission (TRMM) Microwave Imager (TMI), The Aqua Advanced Microwave Scanning Radiometer for EOS (AMSR-E) for their global data assimilation, and further developments and enhancements are in progress. In the European Centre for Medium-Range Weather Forecasts (ECMWF) NWP system, the microwave radiance data from SSMIS, TMI, and AMSR-E have been assimilated directly in all-sky conditions. In regional data assimilation, Japan Meteorological Agency's (JMA) Meso-scale NWP system utilizes the microwave imager radiances in clear conditions and retrieved precipitation from the radiances are assimilated in rainy conditions (Kazumori, 2014). The assimilation of the microwave imager data in all weather conditions can improve the accuracy of humidity and cloud analysis and also benefits forecasts. Accuracy of radiative transfer model is one of the key elements for the radiance assimilation. Furthermore, continuity of utilization of microwave imagers is crucial for operational NWP centres to maintain the accuracy of the initial field for forecast models. In this paper, recent improvement in ocean emissivity modelling in the radiative transfer model and development for introduction of new microwave imagers (GCOM-W1/AMSR2 and GPM/GMI) into NWP systems are described.

2 Ocean Emissivity Model

Ocean emissivity is determined by sea surface temperature, salinity, foam and surface roughness. An accurate microwave ocean emissivity is necessary to assimilate surface sensitive microwave radiances over the ocean. Two-scale models of the ocean surface are suggested. The theoretical models require an integration over the ocean wave spectrum to calculate the microwave ocean emissivity. This calculation requires huge computational costs. In order to use the emissivity model in operational data

assimilation, parameterizations are necessary for fast calculation. In two scales modelling, three parameterizations are used.

- 1) Effects from large-scale wave. Large-scale waves are surface wave with wave length that is long compared to the radiation wave length. Actually, they are a collection of titled facets, each acting as an independent specular surface. The effects are parameterized as functions of incidence angle, wind speed, sea surface temperature and frequency.
- 2) Effects from small-scale wave. Small-scale waves are on top of the large scale waves. The small scale waves are capillary waves. The wave length is small compared to the radiation wave length.
- 3) Sea foam and whitecap effects which are generated by ocean surface wind. The sea foam and whitecap are parameterized with fractional coverage and foam emissivity which depend on incidence angle and surface wind speed.

Except for low frequency channel's observation (i.e. L band channel), effects of salinity are negligible. In fast radiative transfer models (e.g. RTTOV, CRTM) for the radiance assimilation, a Fast Emissivity Model (FASTEM) is utilized to calculate ocean emissivity.

In the FASTEM, specular ocean surface emissivity for calm ocean case is calculated. This part is the dominant part of ocean emissivity and can be calculated by Fresnel formula. This part depends on frequency, incidence angle, sea surface temperature, salinity and dielectric constant of sea water. A correction which represents the effect of small scale waves is applied. This correction is isotropic. The obtained emissivity includes wind-induced emissivity increase. Moreover, adjustments including the effects from the large scale waves are applied. These are parameterized as function of wind speed and incidence angle empirically. Furthermore, effects from foam and whitecap are incorporated with the fractional coverage and foam emissivity which are expressed as function of incidence angle and surface wind speed.

Azimuthal variation corrections (relative wind direction effect) are included in the FASTEM. This part is expected to represent microwave radiance dependence on surface wind direction relative to the sensor azimuthal look. However, this function had not been used operationally because it was thought that the effect of the azimuthal variation was relatively small compared to other biases (e.g. wind speed, frequency, etc.). It should be noted that the effect becomes large, especially under high wind speed condition. Recent improvements in accuracy of first guess field from NWP model reveal the biases from non-modelling of the azimuth variation. An azimuthal variation of the ocean emissivity was developed and their necessity is discussed in Kazumori and English (2014). The model is implemented in RTTOV as FASTEM-6. The azimuthal variation of the microwave radiance depends on relative wind direction (RWD) and surface wind speed. Figure 1 shows comparison of the new azimuthal model in the RWD space. The new model clearly shows better performance than other azimuth emissivity model in FASTEM.

Kazumori and English (2014) showed the performance of the new model in microwave imager assimilation. Figure 2 indicates mean root mean square (RMS) difference of 1000 hPa specific humidity analysis increment between Tests and Control. In the Control run, azimuth emissivity model is not used for microwave imagers. Test1 (shown in panel (a)) uses the new azimuth emissivity model and Test2 (panel (b)) uses FASTEM-5 azimuth emissivity model for microwave imagers (AMSR-E, TMI, and SSMIS). The experiment period is from 20 June to 3 October 2011. The experiment was performed with ECMWF system as of June 2013. The results show reduction in humidity analysis increment in high wind speed and low wind direction variability areas. The result from the new

azimuth emissivity model indicates that the new model has right sensitivity which needs to make consistent changes in the initial state. The experiment results clearly showed the importance of the modelling of the azimuthal variation in the microwave radiance assimilation.

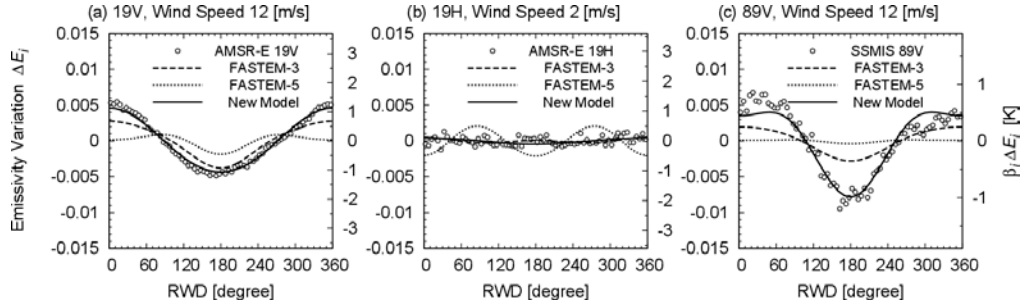


Figure 1: Comparisons of observed azimuth variation of the radiance and RWD models: (a) is AMSR-E 19V at wind speed 12 m s^{-1} ; (b) is AMSR-E 19H at wind speed 2 m s^{-1} ; (c) is SSMIS 89V at wind speed 12 m s^{-1} .

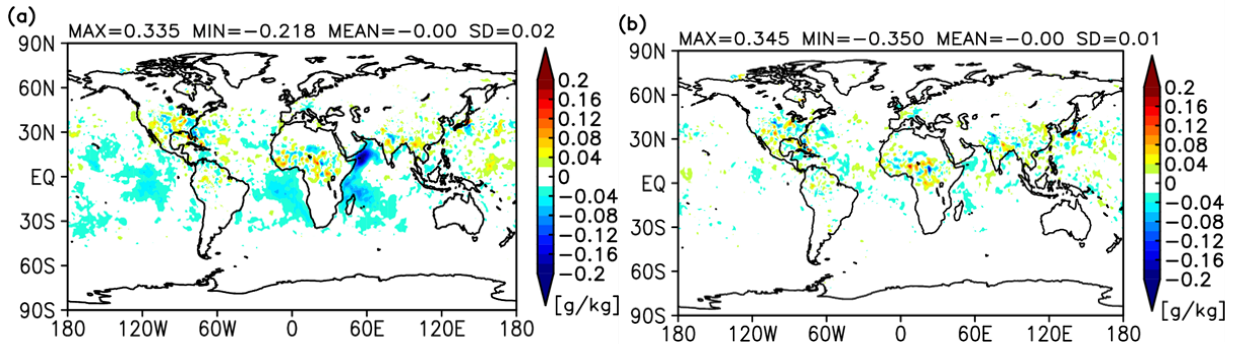


Figure 2: Mean RMS difference of 1000 hPa specific humidity analysis increment between the Test run and the Control run: (a) is Test1 and (b) is Test2. Blue colours indicate a reduction in the analysis increment in the Test runs. The units are in g kg^{-1} .

3 GCOM-W1/AMSR2

GCOM-W1/AMSR2 is the only microwave imager in the A-Train orbit and no other microwave imager in the same orbit is planned, so it is expected to fill a temporal and spatial gap in coverage and hence its assimilation should bring improvements in analyses and forecasts. Data quality assessment was performed based on FG (First Guess) departure statistics in the ECMWF system (Kazumori et al., 2014). The three microwave imagers (AMSR2, SSMIS, and TMI) showed comparable standard deviations of FG departure. The results indicate noise levels in the observations are similar. AMSR2 radiance data quality is comparable to other microwave imagers. Horizontal distribution of AMSR2 FG departure which is normalized with observation errors used in the ECMWF system revealed biases that only occur under certain meteorological conditions. They seem to originate from issues in the forecast model and radiative transfer model performance. The spatial and temporal patterns of the biases are common among the microwave imagers. Figure 3 shows the mean normalized FG departures of assimilated AMSR2 radiances for 37 GHz V channel. Similar biases exist in other

channels. To examine characteristics of the biases, the FG departure data were separated for ascending data and descending data. This separation helps investigation on biases that are dependent on local time.

3.1 Biases in high surface wind speed and low wind direction variability areas

In Figure 3, the sign of the biases in the Arabian Sea (along Somali jet) is different between the orbits, although mean standard deviations of FG departure are smaller (not shown) compared to other regions.

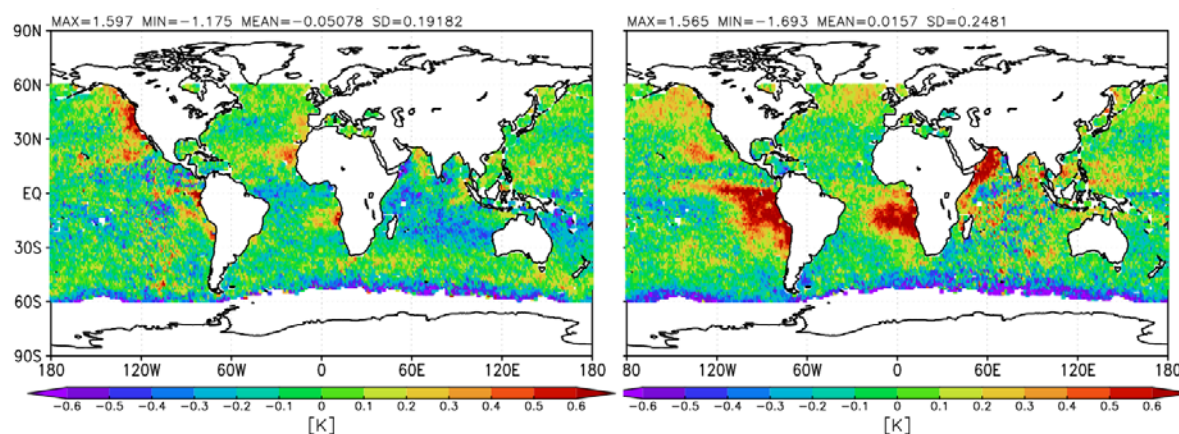


Figure 3: Normalized mean FG departure distributions of assimilated AMSR2 data. The period for the statistics is from 15 July to 15 October, 2013. The results are AMSR2 are 37 GHz V channels. The left panels indicate ascending orbit data (local time 13:30), the right panels indicate descending orbit data (local time 1:30).

As mentioned earlier, the effects of relative wind direction on ocean surface emissivity has not been modelled in these FG departure calculation yet. The biases in the Arabian Sea are caused by these issues, but they can be substantially reduced if the new RWD emissivity model of Kazumori and English (2014) is applied.

3.2 Biases in cold sectors

Positive and negative biases of microwave imager's FG departure in high latitude areas in the southern hemisphere exist in the ECMWF system. The biases can be seen in both ascending and descending orbit data. Figure 3 shows results of after a quality control (removal of positive biased data in cold sectors). Most of the positive biased data can be removed by quality control processes.

3.3 Positive biases in stratocumulus areas and their diurnal variations

Furthermore, Figure 3 shows clear positive biases west of the continents in the tropics. The biases are larger in descending orbits (night-time observations). These areas typically have large-scale marine stratocumulus clouds. The variability of the stratocumulus cloud shows liquid water path (LWP) diurnal variations. The temporal and spatial variability of the cloud properties; i.e., LWP, cloud top height, and cloud thickness must be modelled correctly in general-circulation models (GCMs). Their radiative properties (i.e. reflection of incoming shortwave radiation with high albedo and emission of long-wave radiation) affect Earth energy balance and are one of the uncertainties in climate simulations. The amount of subtropical marine stratocumulus is usually underestimated in GCMs.

The ECMWF all-sky assimilation system monitors the FG departures of microwave imagers on various sun-synchronous polar orbit satellites (AMSR2/GCOM-W1, SSMIS/DMSP F18, F17, F16, and WindSat/Coriolis) and one non sun-synchronous satellite (TMI/TRMM). Using these FG departure data, it is possible to examine the model biases in the stratocumulus areas. The biases of the FG departure show a dependency on observation local time. Top panels in Figure 4 and Figure 5, for the summer and winter cases, show mean FG departure horizontal distributions of AMSR2 37 GHz V channel for areas characterized by marine stratocumulus (area (a)), as well as for nearby areas where stratocumulus is uncommon (area (b)).

The biases in summer are larger than those in winter cases. The biases tend to be limited to typical marine stratocumulus cloud areas. For the two areas referred to as (a), (b), Figure 4 (a), (b) and Figure 5 (a), (b) show the area averaged FG departure from the microwave imagers. Microwave imagers on polar orbiting satellites can provide two results per day. TMI can provide various local time statistics for the experiment period. The bias behaviour in area (a) shows diurnal variation following the LWP amount itself. The bias variations were consistent among the microwave imagers, and could not be found in area (b). The biases in 19 GHz V and 23 GHz V channels are plotted for comparison as well. The biases in 37 GHz V are larger than those of other channels. Because 37 GHz channels have higher sensitivity to LWP than other channels, the results suggest LWP in the FG is underestimated in the night-time. In the stratocumulus areas, the LWP diurnal variation from the model is underestimated and the model's LWP amount is insufficient. Comparison with other independent LWP L2 products from Remote Sensing Systems showed that amplitude of the LWP diurnal variation in the model is smaller than that of their retrieved L2 products.

4 GPM/GMI

Global Precipitation Measurement (GPM) is a joint mission of JAXA and NASA. The GPM core satellite was launched on 27 February 2014. GPM uses a core satellite (GPM satellite) and constellation satellites to produce 3-hourly global precipitation map. GPM core satellite has two sensors. They are GMI (GPM Microwave Imager) and DPR (Dual Precipitation Radar). GPM satellite takes over a role of TRMM satellite in precipitation measurement. Because GPM satellite uses a non-sun-synchronous orbit and a high inclined orbit, GMI can observe high latitude area. Therefore, GMI data coverage is wider than those of TRMM/TMI. Furthermore, GMI has new observation channels, (i.e. 166 GHz V and H polarization and two water vapour sounding channels at 183 GHz). These are new key features for the data utilization in NWP.

Preliminary assimilation experiments were performed in JMA Meso-scale NWP system. Main target of JMA Meso-scale NWP system is accurate precipitation forecasts for Japan and its surrounding areas. Non-hydrostatic model (JMA-NHM) and non-hydrostatic model based 4D-Var are used for the assimilation experiment. Microwave imager data are assimilated in the system (Kazumori, 2014). In clear sky condition, microwave radiance data are assimilated. In precipitation area, retrieved rainfall intensity data are assimilated. The radiance data from 19, 23, 37, 89 GHz vertical polarized channels are assimilated. The experiments were performed for a heavy precipitation event in Japan. The control experiment was same as JMA operational Meso-scale NWP system. The test experiment includes GMI data in addition to the control experiment. The data assimilation period was for July 1 to 11 in 2014. In the experiment period, there was a heavy rain event in Kyushu (western island of Japan). Figure 6 shows the surface weather chart and MTSAT infra-red imager for the time.

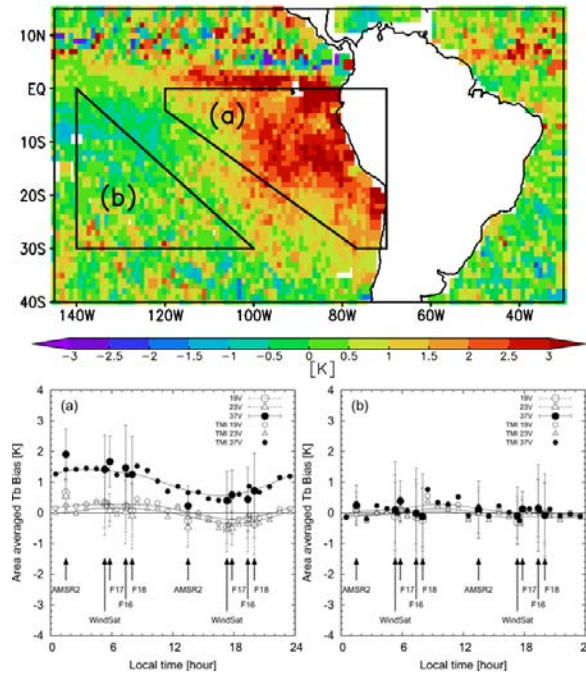


Figure 4: Area averaged FG departure biases in the summer experiment period. The area for averaging is plotted in top panel with AMSR2 37 GHz V mean FG departure map. The focused areas (a) and (b) are shown with surrounded area with black lines. Bottom panels show the biases as functions of observation local time of microwave imagers (AMSR2, SSMIS F16, F17, F18, WindSat, and TMI). TMI biases are shown with smaller symbols. White circle is 19 GHz V, white triangle is 23 GHz V, and black filled circle is 37 GHz V biases. Bars indicate the standard deviations.

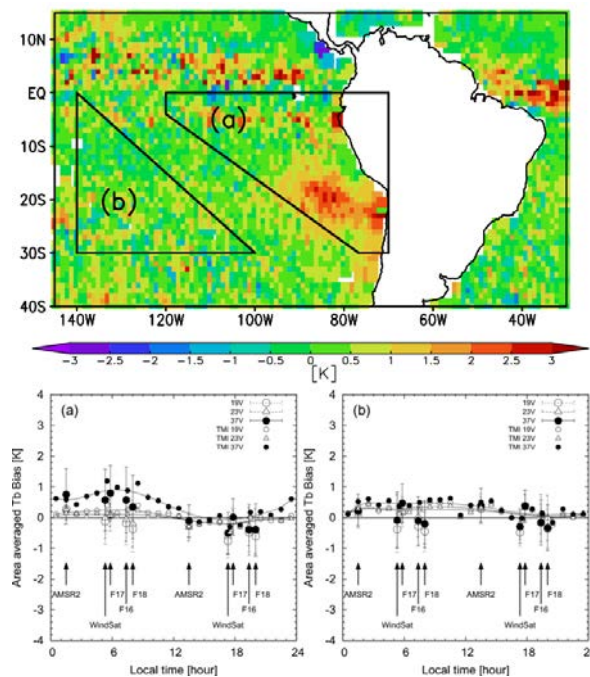


Figure 5: As Figure 4 but for the winter experiment period.

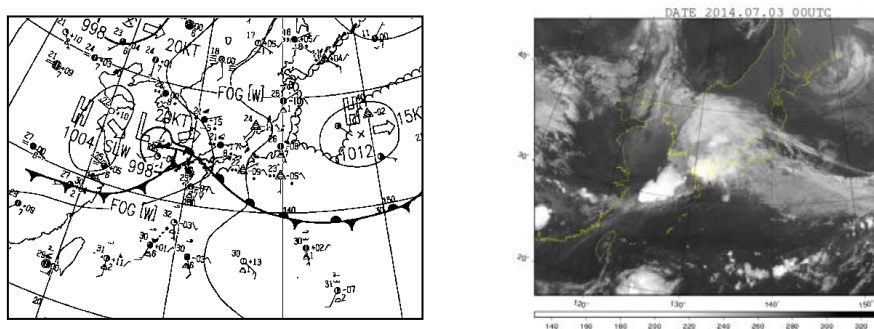


Figure 6: Surface weather chart for Japan area (left panel) and infra-red MTSAT imager (right panel) on 00 UTC on July 3, 2014.

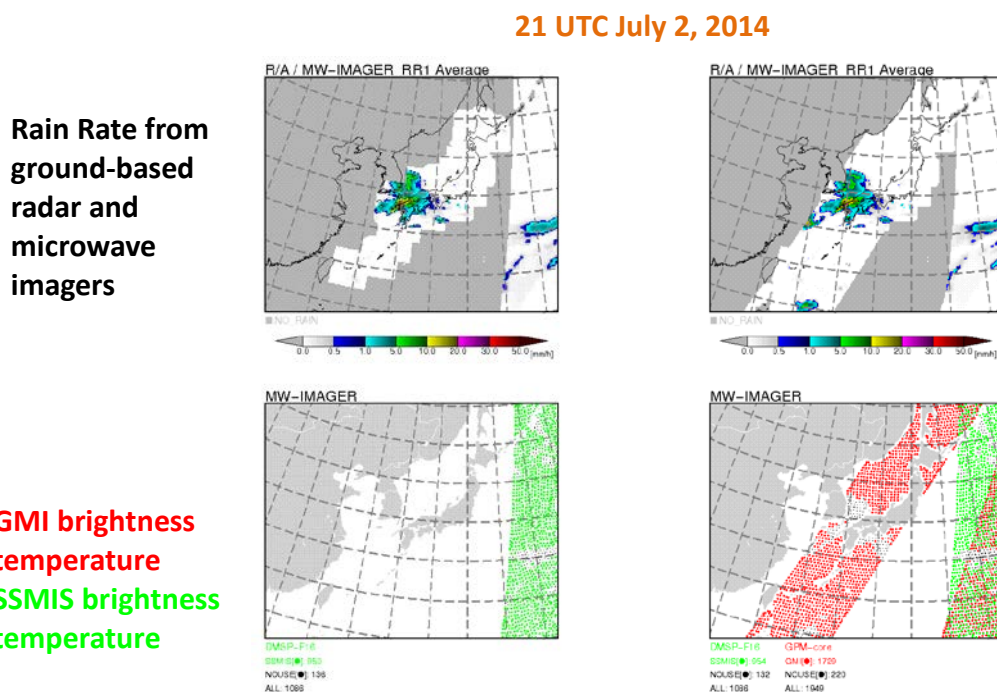


Figure 7: GMI data coverage for 21 UTC on July 2, 2014 analysis. Top panels are retrieved precipitation and bottom panels are microwave imager’s brightness temperature data. Left panels show the coverage without GMI data and right panels shows that with GMI data.

Figure 7 shows examples of GMI data coverage in 21 UTC July 2, 2014. The GMI data can fill the gap in microwave imager data (AMSAR2, three SSMIS (F16, F17, and F18) and TMI are used in the system)

An improved precipitation forecast with GMI data assimilation is shown in Figure 8. From comparison with radar observation, the assimilation of GMI data improved precipitation forecasts in the JMA Meso-scale system.

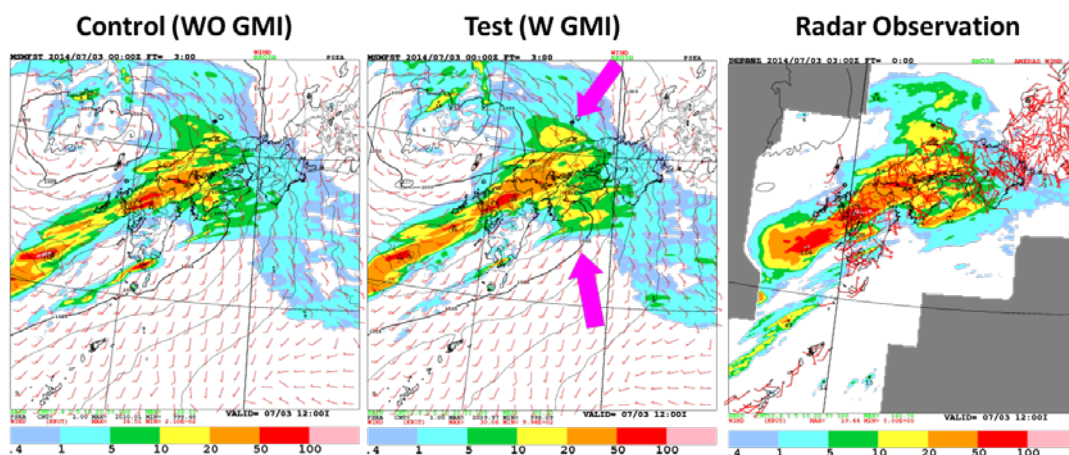


Figure 8: Three hour accumulated precipitation forecast, surface wind field, and sea level pressure from 00 UTC on 3 July 2014. Left panel indicates the forecast without GMI data, middle panel indicates the forecast with GMI data. Right panel shows the observed precipitation by ground based radar and surface wind observation.

5 Summary and future prospect

Microwave imager observations provide information on various geophysical parameters. They are essential data for initialization of NWP models. The data can be utilized for NWP model evaluation.

Accuracy of microwave radiative transfer model is a key element for the data assimilation. Recently, improved microwave ocean emissivity model was developed to include azimuthal brightness temperature variation over oceans. The emissivity model is adopted as FASTEM-6 in RTTOV. New microwave imager data are available and their utilization is in progress. Investigation on AMSR2 and other microwave imager's FG departure in the ECMWF system showed biases which were related with radiative transfer model and forecast model itself. For enhanced utilization of microwave imager data, it is necessary to reduce the biases with improved radiative transfer model as observation operator and forecast model improvement. Addition of GPM/GMI data into JMA Meso-scale NWP system filled gaps in microwave imager data coverage in the system. The assimilation of GMI data brought humidity increments in the system and accurate precipitation forecasts.

Finally, low frequency channels (6 and 10 GHz) are not yet fully explored in the microwave imager assimilation. From their data assimilation, the atmospheric signal and surface signal can be obtained together under rainy and/or strong surface wind situation. The assimilation could provide further improvement in precipitation forecast.

References

- Kazumori, M., 2014: Satellite radiance assimilation in the JMA operational mesoscale 4DVAR system, *Mon. Weather Rev.*, **142**, 1361–1381.
- Kazumori, M. and S.J. English, 2014: Use of the ocean surface wind direction signal in microwave radiance assimilation. *Q. J. R. Meteorol. Soc.*, in press. DOI:10.1002/qj.2445.
- Kazumori M., A.J. Geer and S.J. English, 2014: Effects of all-sky assimilation of GCOM-W1/AMSR2 radiances in the ECMWF system, *ECMWF Tech. Memo. No. 732*, pp. 34.